9

Porous Ceramic Matrix Al_2O_3/Al Composites as Supports and Precursors for Catalysts and Permeable Materials

S.F.Tikhov[1], N.A.Pakhomov[1], E.I.Nemykina[1], A.N.Salanov[1], V.A.Sadykov[1], V.E.Romanenkov[2] and Ya.Ya. Piatsiushyk[2]
[1]*Boreskov Institute of Catalysis RAS, Novosibirsk*
[2]*Powder metallurgy institute NAS Belarus*
[1]*Russia*
[2]*Belarus*

1. Introduction

Al/Al_2O_3 composites are widely regarded as promising construction materials (Yun et al., 2002; Watari et al., 2000; Saiz & Tomsia, 1998). Methods used for production of such materials traditionally include high-temperature processing. As a result, such materials have a low porosity and can not be used in adsorption and catalytic processes.

Meanwhile, permeable systems based on porous powder materials (PPM) – metals or oxides, are widely used as supports for catalysts and membranes (Sabirova et al., 2008; Ismagilov et al., 1997; Lee, 2003; Wang et al., 2004; Vityaz et al., 1987). When combined with catalysts (catalytically active components), permeable materials manufactured as membranes can substantially change selectivity to products of catalytic reactions (Rohde et al., 2005). Unfortunately, the amount of the active component that can be incorporated into traditional PPM is limited by poorly developed microporous and mesoporous structure of such materials. Porosity also declines during high-temperature processing required for production of mechanically durable products. For example, specific surface area of ceramic membranes based on alumina does not exceed 9 m^2/g with average diameter of macropores about 0.12 μm (Ismagilov et al., 1997). The specific surface of PPM and metal powders is significantly lower. Attempts of increasing the mesoporous component in PPM prepared from metal powders by filling macropores with suspensions resulted in substantial decrease of the average size of transport macropores and PPM permeability (Wang et al., 2004).

It was shown earlier that during hydrothermal oxidation (HTO) aluminum-containing powders are cemented into a robust macroporous monolith with relatively high specific surface area due to partial aluminum oxidation by water (Tikhov et al., 2005). During calcination the formed aluminum hydroxides are decomposed yielding nano(meso)porous component in Al_2O_3/Al ceramometals (cermets) localized in their oxide ceramic part. Particles of remaining aluminum are evenly distributed in the oxide matrix. A typical relief of the fracture face of Al_2O_3/Al cermet prepared by oxidation of aluminum powder by water at 100°C followed by calcination in air at 550°C is shown in Fig. 1. One can see that aluminum particles are covered by a porous oxide film.

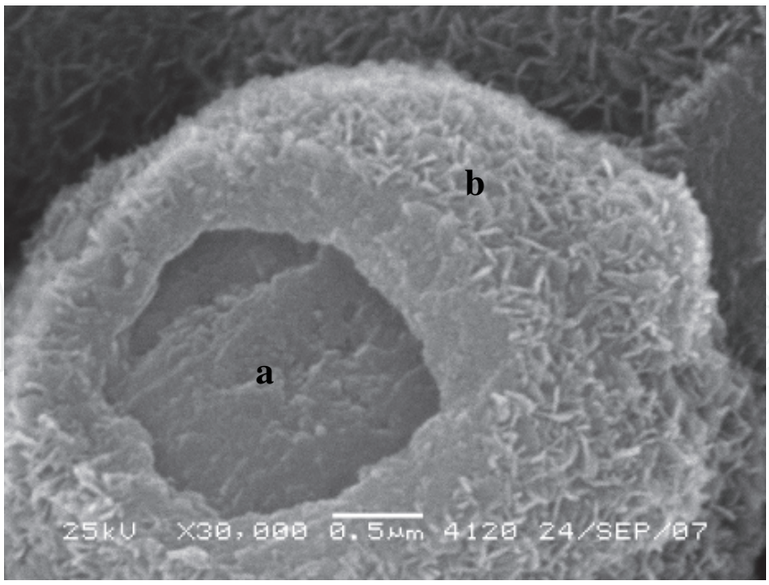

Fig. 1. SEM micrograph of Al_2O_3/Al cermet prepared from ASD-4 powder: a – aluminium core, b - porous alumina matrix.

Depending on the degree of aluminium oxidation during HTO and calcination temperature, the nano- and macroporous structure of the materials can be varied in a broad range (Tikhov et al., 2004; Rat'ko et al., 2004). The macroporous structure and permeability of the porous composites can be varied by changing the size and shape of the aluminum precursor particles. In addition, the mesoporous structure of aluminum oxide in the cermets can be tuned by mixing aluminum powder with aluminum oxides or hydroxides (Tikhov et al., 2004). In this paper we shall report the results of studying the properties of permeable cermets prepared from aluminum powders PAP-2, ASD-1 (Tikhov et al., 2004), ASD-4 and a mixture of aluminum powder PA-4 with the product of gibbsite thermal activation (Zolotovskii et al., 1997). The effects of the synthesis parameters on structural-mechanical and catalytic properties of cermets in isobutane dehydrogenation will be discussed.

2. Phase composition of Al_2O_3/Al composites

Typical XRD patterns of Al_2O_3/Al cermets are presented in Fig. 2. They include intense narrow peaks corresponding to 111, 220, and 200 reflections of aluminum phase. In addition, the XRD patterns contain weak broad peaks corresponding to 311, 400, 511, 440 reflections of aluminum oxide spinel phase [Tsybulya & Kryukova, 2008]. The phase composition of the aluminum oxide can not be characterized in more detail due to its poor crystallinity.

A comparison of the intensity of 440 peak of Al_2O_3 with that of 220 peak of Al shows (Fig. 2) that the content of aluminum oxide in the Al_2O_3/Al composites grows in the sequence: ASD-1<ASD-4<PAP-2. Quantitative estimates of the oxide content based on the earlier reported calibration curve (Tikhov et al., 2004) are shown in Table 1.

The differences of the oxide content in cermets are mostly due to different reactivity of the used aluminum powders at the initial hydrothermal oxidation stage (Tikhov et al., 2007). Aluminum is practically not subjected to any oxidation during calcination in air at 550°C. Hence, variation of the aluminum reactivity with respect to water allows to tune the content of the oxide phase in the Al_2O_3/Al cermets.

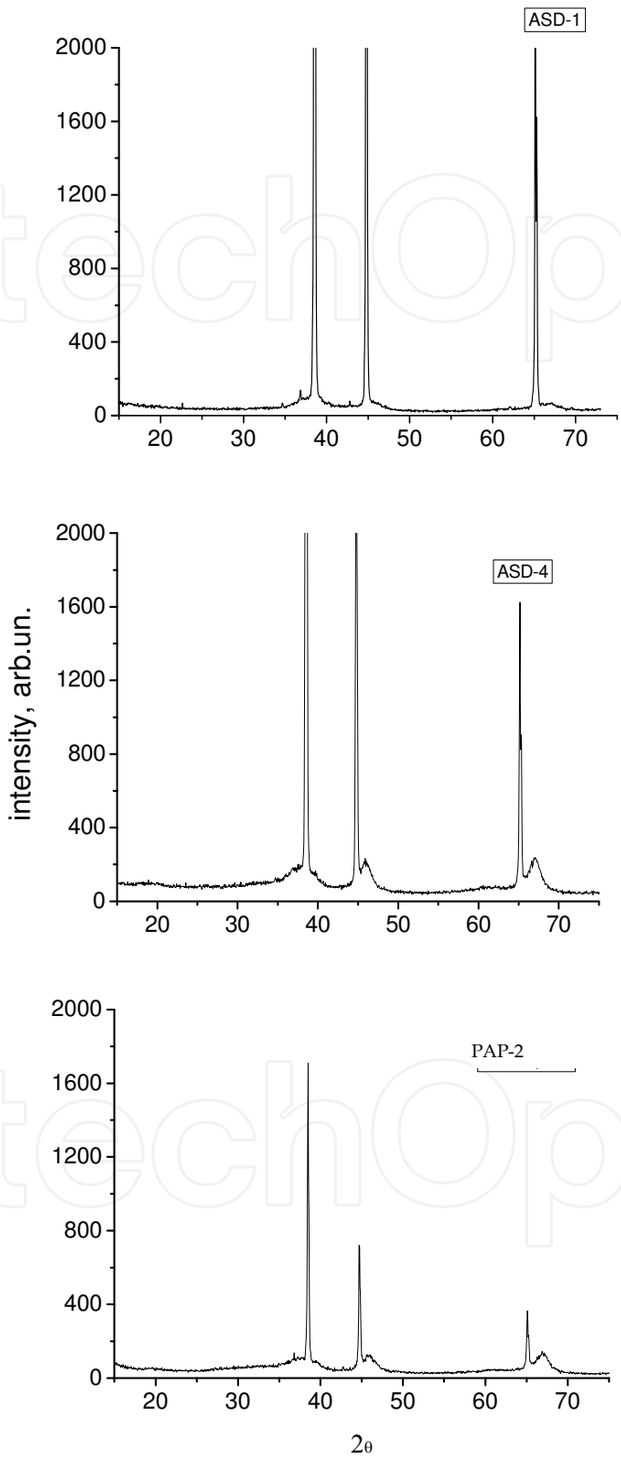

Fig. 2. XRD patterns of Al_2O_3/Al cermets prepared from different aluminum powders.

3. Macropore structure and permeability of cermets obtained from different aluminum powders

Qualitative analysis of the cermet macrostructure (Fig.3a,b,c) shows that it substantially depends on the type of the aluminum powder. The loosest packing of the monoliths is typical for cermets produced from PAP-2 powder. Averaged characteristics of the obtained materials estimated by the Darcy and "bubble point" methods (Vityaz et al., 1987; Khasin, 2005) using supports in the form of porous disks made of PTK-grade titanium foam (average pore size 120 μm, diameter 30 mm) containing the studied cermet deposited on their external surface by HTO followed by calcination are also very different (Table 1). The average pore diameter determined by this method increases from 1 to 22 μm in the series of cermets ASD-4<ASD-1<PAP-2. The maximum pore size varies in a similar order. The permeability coefficients of obtained materials also differ by more than a factor of 50 correlating with the average pore size (Table 1).

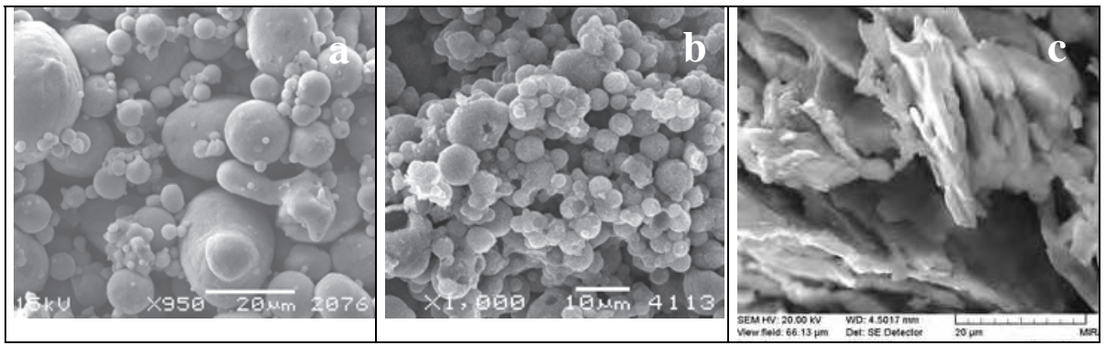

Fig. 3. SEM micrographs of porous Al_2O_3/Al composites prepared from different aluminum powders: (a) - ASD-1, (b) – ASD-4, (c) – PAP-2. (LEO 1455VP ,"Tescan"; JEOL JSM-6460V).

Comparison of the macropore structure parameters (Table 1) with a qualitative analysis of the macrotexture (Fig. 3) shows that a decrease of the average size of cermet particles aggregates decreases the average size of macropores and permeability. The average size and shape of particles in cermets are determined by the particles of the aluminum source powder used for synthesis. According to the data obtained by the Koulter method, the average particle size changes as follows: ~ 33 μm (ASD-1), ~ 12 μm (ASD-4), ~ 5 and ~ 35 μm (PAP-2) (Table 1). This trend qualitatively matches the results obtained by SEM (Table 1, Fig. 3). Larger average particle sizes obtained by the Coulter method for ASD-1 and ASd-4 samples in comparison with the SEM data are due to partial aggregation of the aluminum powder during its preparation or storage. Substantial variation of the particle size obtained for PAP-2 is, most likely, due to the flat shape of the particles that are also partially aggregated.

The differences in the shape and average sizes of porous cermet particles are quantitatively expressed in the loading density of aluminum powder in a die before HTO. For example, the loading density is about 1.6-1.8 g/cm^3 for ASD-4, about 1.3-1.4 g/cm^3 for ASD-1 and about 0.3-0.4 g/cm^3 for PAP-2. In turn, the loading density is largely determined by the size and shape of aluminum particles. The flat shape of partially aggregated PAP-2 particles is known to result in substantially lower filling density compared to round particles (Tikhov,

2004 [8]). Round particles typical for ASD-1 and ASD-4 aluminum source (Tikhov et al., 2004) provide for a denser packing. Apparently, different particle packing is also preserved in the obtained cermet monoliths (Fig. 3). As the result, the average size of macropores in PAP-2 monolith is substantially larger. The composite obtained from ASD-4 has the smallest pore size. This is determined by the dimensions of cavities between the aluminum particles that are much larger for ASD-1. The degree of aluminum conversion to hydroxide determining the fraction of oxide in Al_2O_3/Al cermets has comparatively minor effect on the parameters of the macropore structure (Table 1).

Source aluminum powder	Average particle size of Al^0, μm	Permeability coefficient, $K\times10^{-13}$, m^2	Maximum macropore size, μm	Average macropore size, μm	Crushing strength, (σ), MPa	Al_2O_3, wt.%	Cermet porosity (ε),%
ASD-1	33*(25)**	~3.5	12.5	6.5	11	~24	~36
ASD-4	12(5)	0.4	4.5	~1	12	~44	~57
PAP-2	~5.4, 35	20	~63.5	22	23	~94	~42

* Coulter method.
()** According to SEM.

Table 1. Macropore structure, permeability and mechanical properties of Al_2O_3/Al composites prepared from different aluminum powders.

Thus, depending on the particle shape, the character of the macropore structure and permeability of the composite materials prepared using hydrothermal aluminum oxidation can be substantially varied.

A comparison with known permeable systems (Khasin, 2005) shows that smaller pores about 5-8 μm are formed when copper powder is strongly pressed together with combustibles. This pore size corresponds to permeability coefficient about 10^{-14}-10^{-13} m^2. The permeability coefficient of macroporous ceramic supports prepared by extrusion of pastes containing aluminum hydroxides and α-Al_2O_3 powder followed by calcination at 1200°C was estimated to be about ~10^{-14} m^2 (Ismagilov et al., 1997). Furthermore, the mechanical strength of ceramics (~0.8 MPa) proved to be substantially lower than that of PAP-2 monolith. This result opens great prospects for production of permeable materials with complex geometrical shapes from aluminum powder.

4. Mechanical properties of cermets

Dependence of crushing strength (σ) on porosity (ε) for PPM is expressed by Balshin's empirical relation (Leonov et. al., 1998; Balshin, 1972):

$$\sigma = \sigma_0 (1-\varepsilon)^m , \quad (1).$$

Here m is the ratio of the total mass of the material to its mass subjected to the mechanical loading; σ_0 is the crushing strength of a non-porous body of the same composition. Equation (1) reflects a well-known trend that the strength of solids decreases when their

porosity grows. This relation is valid for most porous cermets prepared using the HTO stage (Tikhov et al., 2000a; Tikhov et al., 2004a; Tikhov et al., 2004b). However, a comparison of the porosity and strength values reported in Table 1 suggests that the Balshin's relation is not valid for this PPM series. In particular, the cermet prepared from ASD-1 is approximately as strong as that made from ASD-4 despite substantially different porosity.
Most likely, this effect is related to a substantial difference in the character of contacts between particles forming PPM. According to (Rebinder et al., 1965), the crushing strength of a porous material (σ) is proportional to the number of contacts between particles (N), the surface area of the contact (S_i) and mechanical strength of the contact unit surface area (σ_i):

$$\sigma = N \cdot S_i \cdot \sigma_i \qquad (2).$$

Apparently, the Balshins's relation is valid only when one or several parameters of Eq. (2) vary only slightly. An abrupt change of parameters N,S,σ related to changes of the size or shape of particles forming a porous composite, or their chemical composition may lead to a substantial deviation from Eq. (1). In our system such deviation may be caused either by the change of the particle diameter from 20 to 5 μm or by change of the particle shape from spherical to flat. Moreover, it is very likely that the surface area of a singe contact in monolith PAP-2 is substantially larger due to the higher PAP-2 conversion at the HTO stage because these are the HTT products that cement the places of contact between the monolith particles (Rat'ko et al., 2004).

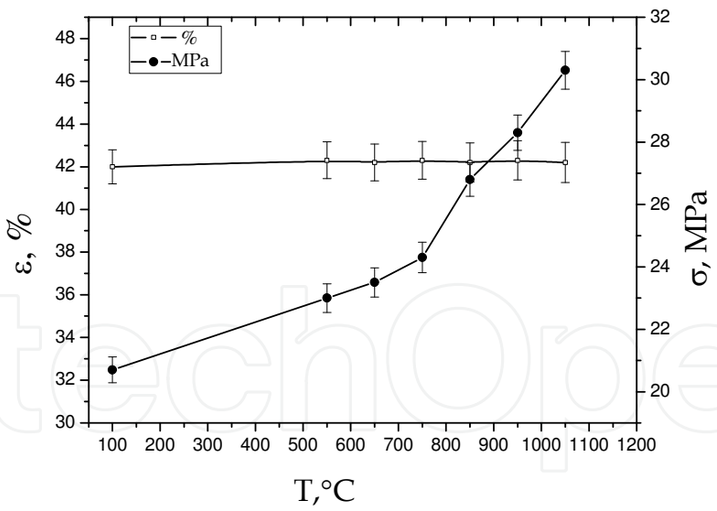

Fig. 4. Dependence of porosity (ε) and crushing strength (σ) on the calcination temperature for Al_2O_3/Al composite prepared from PAP-2.

Another example of a deviation from the Balshin's relation is a weak dependence of the crushing strength on porosity when the temperature of preliminary calcination of the ceramic granules increases (Fig. 4). In this case high-temperature sintering may also lead to the growth of contact surface area due to the surface diffusion or strengthening of a single contact due to its better crystallization.

Overall, one should take into account that porous ceramic supports, which are chemically the closest analogs of our materials, usually have substantially lower mechanical strength at comparable parameters of the macropore structure (Ismagilov et al., 1991). So, ceramometallic PPM with the aluminum oxide matrix may have great prospects in various applications.

5. Specificity of the nanopore structure of cermets

One of the most remarkable properties of composites prepared by cementing aluminum-containing powders under hydrothermal conditions is the presence of developed nano (micro, meso) porous structure formed by primary aluminum oxide nanoparticles and their aggregates. These particles are formed during thermal decomposition of aluminum hydroxides obtained from aluminum metal particles at the HTO stage. Qualitatively, differences in the size and shape of nanoparticles can be seen even in SEM images despite substantial limitations in resolution (Fig. 5). The largest aggregates of particles are typical for PAP-2. Meanwhile, the smallest particle size (< 0.1 μm in diameter) is observed for ASD-4. The aggregates of the oxide formed from ASD-1 have an intermediate size.

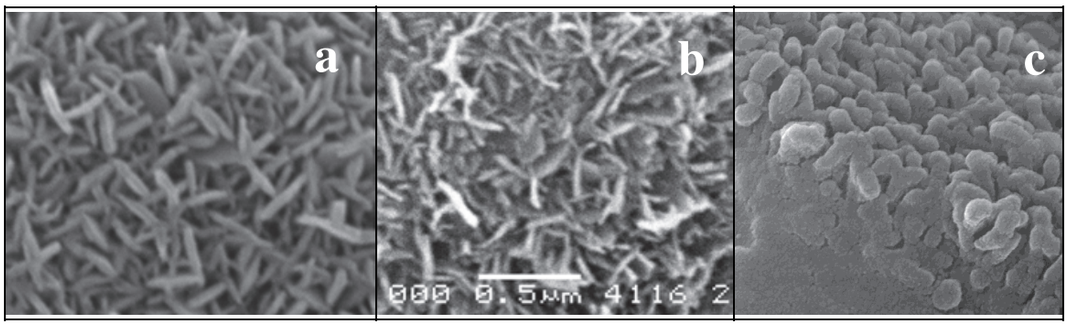

Fig. 5. Specificity of the microstructure of alumina aggregates on the surface of aluminum particles inside Al_2O_3/Al cermets prepared from different powders according to SEM data: (a) – ASD-1, (b) – ASD-4, (c) – PAP-2.

Averaged quantitative information on nanopores can be obtained from the analysis of adsorption-desorption isotherms. The isotherm presented in Fig. 6a and the pore size distribution (Fig. 6b) are typical for all PPM synthesized by HTO of aluminum powders and calcined at 500-700°C. According to the IUPAC classification (Gregg & Sing, 1982), the isotherms are close to type II, whereas the capillary condensation hysteresis loops are similar to type H3 (Fenelonov, 2002). The latter is typical to slit-like pores formed by flat parallel particles. The data reported in Table 2 show that the surface area and volumes of PPM nanopores may substantially vary depending on the type of the Al source powder and HTO conditions. At similar calcination temperatures the total surface area and volume of PPM nanopores usually increase when the fraction of highly porous aluminum oxide increases. Therefore, the highest values of these parameters were obtained for PPM prepared from PAP-2 that has ~90% aluminum conversion.

The characteristics of the alumina nanopore structure in the composites can be estimated more precisely with the account of the total specific surface area of the composite (S) and the fraction of oxide in it by calculating the specific surface area of the oxide (S_{Al2O3}) according to Eq. (3).

$$S_{Al2O3}=S_{sp}(1+\alpha X_0)/\alpha(1+ X_0) \quad (3).$$

Here α is aluminum conversion to aluminum oxide, and $X_0 = 0.89$ is the relative weight change of the solid when all aluminum metal is oxidized (Tikhov et al., 2004a). The values of the aluminum oxide specific surface areas reported in parenthesis (Table 2) show that the specific surface areas of the oxide differ substantially for PPM prepared from ASD-1 and ASD-4 despite the fact that their total specific surface areas are similar. This result is largely related to different ratios of the aluminum hydrothermal oxidation rate to the ageing rate of the HTO products under hydrothermal conditions (Tikhov et al, 2000b). The particle dimensions should increase due to recrystallization of nanoparticles when the relative ageing rate increases, whereas the specific surface area should decrease. For ASD-1 and ASD-4 powders the ageing rates determined by the external HTT conditions were approximately equal. Meanwhile, the rates of Al consumption at the second diffusion-controlled stage of hydrothermal oxidation were substantially different. For ASD-4 this rate was higher by two orders of magnitude (Tikhov et al., 2007). Therefore, the smallest hydroxide (oxide) particles were obtained for this PPM. For PAP-2 the lowest oxidation rate was observed in the diffusion region. This led to a significant growth of the primary particle dimensions and decrease of the alumina specific surface area in comparison with the other samples.

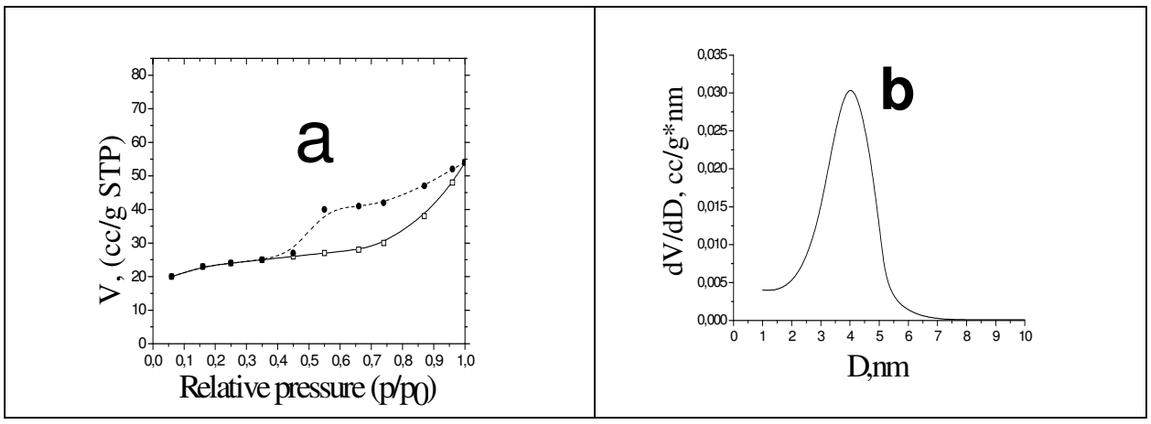

Fig. 6. Adsorption-desorption isotherm (a) and nanopore size distribution (b) for Al_2O_3/Al composite prepared from ASD-4.

Precursor aluminum powder	Specific surface area of Al_2O_3/Al (Al_2O_3), m^2/g	Nanopore volume (V), cc/g	Nanopore diameter, nm	Reference
ASD-1	52 (221)	0.05	3.8	(Tikhov et al., 2004a)
ASD-4	54 (318)	0.05	4.7	-
PAP-2	121 (~121)	0.16	4.7	-

Table 2. Parameters of the nanopore structure of Al_2O_3/Al composites.

The parameters of the nanopore structure are also substantially affected by the calcination temperature of cermets. The results obtained during investigation of the adsorption characteristics of PPM prepared from PAP-2 and calcined at increasing temperatures are reported in Table 3 and Fig. 7. The adsorption isotherms visibly change from type II to type III according to the IUPAC classification. The hysteresis loop practically disappears at high

calcination temperatures (Fig. 7g). This fact is largely related to the changed pore size distribution (Fig. 7 b,d,f,h). Initially the sample had nanopores with a narrow pore size distribution around 4 nm. Additional mesopores with diameter ~ 5 nm appear starting from calcination temperature 850°C. At higher calcination temperatures the relative fraction of the nanopores with the size ~ 4 nm decreases whereas that of the larger pores increases. The average size of these pores grows to 8-10 nm.

The behavior of the specific surface area and volume of nanopores with increasing calcination temperature is somewhat unusual. The initial growth of the specific surface area after the heat treatment at 550°C is due to the thermal dehydration of aluminum hydroxide and formation of Al_2O_3. The pore size does not change during this process. However, the number of nanopores grows as it is indicated by a two-fold increase of the pore volume. Probably, this effect is due to a deviation of the aluminum hydroxide dehydration from an ideal pseudomorphic transformation (Tikhov et al., 2004a; Tikhov et al., 2004b).

Calcination temperature, ^oC	Specific surface area, m^2/g	Nanopore volume, cc/g	Nanopore diameter, nm
120	86	0.07	4.7
550	121	0.16	4.7
650	116	0.16	4.9
750	107	0.16	5.0
850	98	0.21	5.9
950	75	-	-
1050	24	0.12	9.5

Table 3. Influence of the calcination temperature on the nanopore characteristics of Al_2O_3/Al composite prepared from PAP-2.

Subsequently, continuous smooth increase of the specific surface area accompanied by the growth of the average pore size is observed with increasing calcination temperature. Until the calcination temperature of 750°C the volume of nanopores is approximately constant with a minor increase of the pore size. For the sample calcined at 850°C the pore volume substantially grows, decreasing at higher temperatures (Table 3). After calcination at 1050°C the pore volume decreases by almost a factor of two, whereas their diameter increases by the same value. Thus, the specific surface area of samples calcined at 550°C or higher temperatures continuously decreases with calcination temperature. Meanwhile, the changes in the volume of nanopores are not monotonous. Such effects are not typical for aluminum oxide powders. Usually, both the pore volume and specific surface area decrease with the calcination temperature (Khalil, 1998; Zhu et al., 2002). However, for granulated aluminum oxides with a large amount of macropores in some cases a small growth of the total pore volume with the temperature of calcination was observed, while their micropore volume and specific surface area decreased (Boreskov et al., 1951). Such effect is, most likely, due to the specific features of sintering of primary aluminum oxide nanoparticles in granulated ceramics. The mechanism of the nanoparticle sintering may be attributed to "internal" sintering due to surface diffusion (Geguzin, 1984), when the growth of particles and decrease of the free surface energy is not accompanied by the pore structure "densification", so that the total pore volume remains approximately constant. This process is possible due to the growth of nanoparticles and formation of separate particles (dense or low-porous) with sizes substantially exceeding those of nanoparticles present in the initial sample. Adjacent particles merge with such particles.

Thus, variation of the aluminum reactivity and calcination temperature allows one to modify the parameters of aluminum oxide nanostructure in PPM.

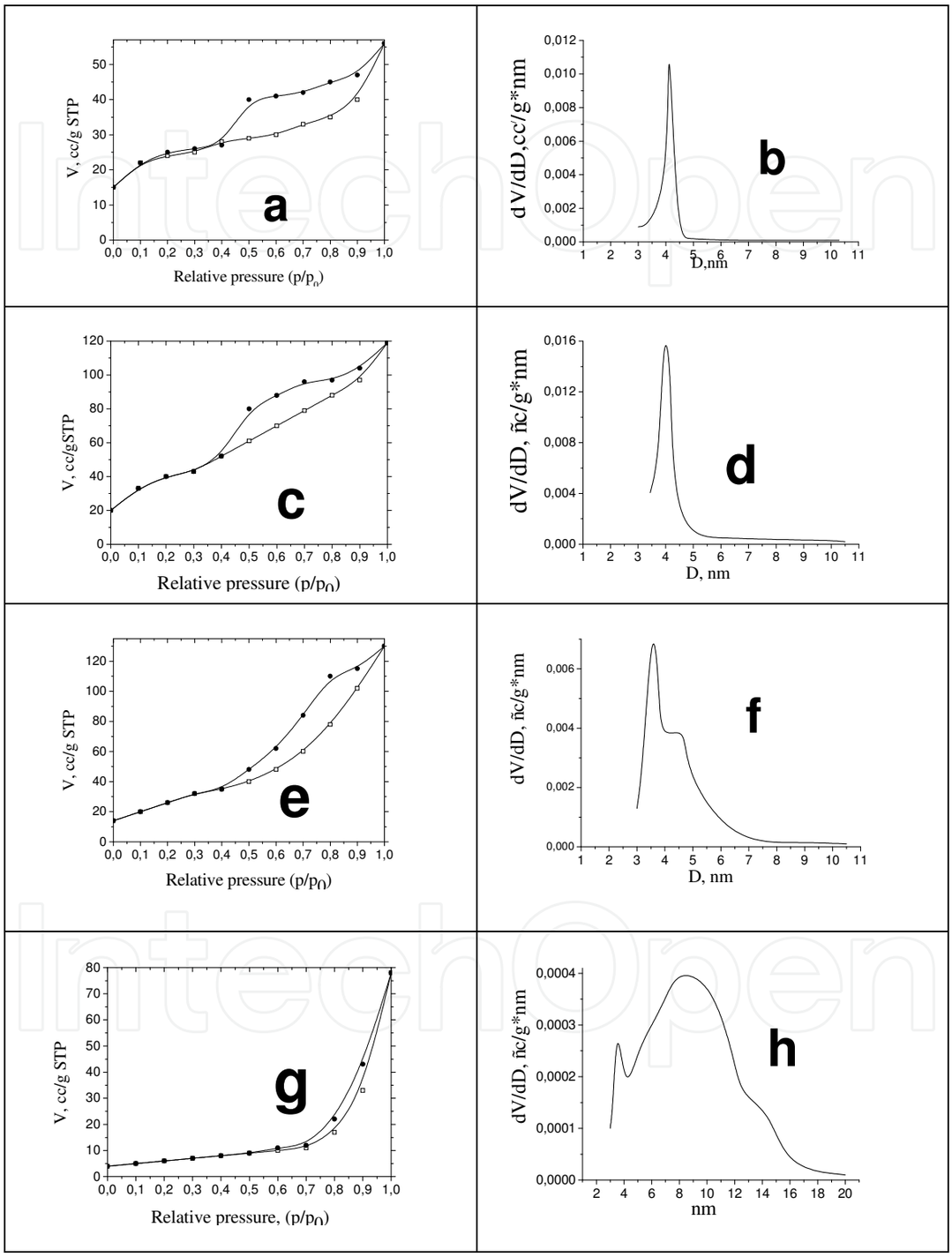

Fig. 7. Adsorption-desorption isotherms (a,c,e,g) and nanopore size distribution (b,d,f,h) of Al_2O_3/Al composite prepared from PAP-2 after different temperatures of calcination: (a,b) – 120˚C; (c,d) – 650˚C; (e,f) – 850˚C; (g,h) – 1050˚C.

6. Nanoporous structure of composites prepared from blends of aluminum with TCA and catalytic properties of the CrO_x/Al_2O_3/Al catalysts in the dehydrogenation of isobutane

Despite the fact that variation of synthesis conditions and type of aluminum powders makes possible to change the properties of nanoporous oxide component in a broad range, their application is substantially restricted by economic and technological problems. In particular, the problems of cost and application safety are the most important for application of cermets as catalyst supports. In this respect, such powders as ASD-1 and similar to it PA-4 are more promising that PAP-2 or ASD-4. The main drawback of the PA-4 powder is a low activity in HTO, which leads to a low surface area and moisture capacity of cermets prepared from it. The last factors are exceptionally important for synthesis of catalysts by impregnation. To improve these parameters, we synthesized supports by blending aluminum powder with the product of gibbsite thermochemical activation (TCA). TCA is amorphous aluminum oxide (Al_2O_3x1.3 H_2O) synthesized by gibbsite dehydration in a pulse mode and characterized by a high chemical activity and ability to be rehydrated to form pseudoboemite in the presence of water vapor (Zolotovskii et al., 1997). During the cermet synthesis TCA is a precursor for additional nanoporous aluminum oxide incorporated in the cermet macropores.

The XRD patterns of the Al_2O_3/Al cermet prepared from a PA-4 + TCA blend and alumina prepared from TCA are shown in Fig. 8. The aluminum oxide concentration in this cermet is higher compared with those where all alumina was obtained by aluminum oxidation (compare Figures 2 and 8). The structure of aluminum oxide both in the composite and in pure aluminum oxide are close to that of γ-Al_2O_3 (Tsybulya & Kryukova, 2008).

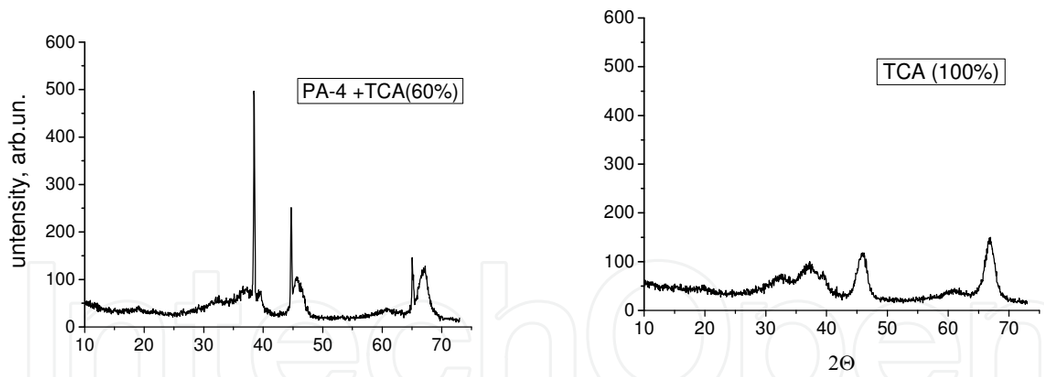

Fig. 8. XRD patterns of Al_2O_3/Al cermet prepared from blend of PA-4 + TCA and alumina from TCA.

Catalysts from Al_2O_3/Al cermets were prepared by incipient wetness impregnation of their calcined granules (3x3 mm cross-section and 3-5 mm length, Fig. 9) with solutions of active component precursors – chromic anhydride and promoters (Pakhomov et al., 2008). In this Chapter we shall report textural properties of the composite supports and catalytic properties of chromium-alumina catalysts in dehydrogenation of isobutane.

Comparison of Figures 1 and 10 proves that the surface texture of cermets prepared with TCA differs substantially from that of cermets without its addition. Primarily, this is a result of introducing a large amount of aluminum hydroxide with aggregates of irregular shape (Fig. 10a). Another reason for the differences in the surface shape is the high

calcination temperature (700°C) favoring aluminum melting from the nanoporous ceramic spheres formed during HTO and calcination (Fig. 10b).

Fig. 9. General view of granulated Al_2O_3/Al composites prepared from powdered TCA and PA-4 used as supports for dehydrogenation catalysts.

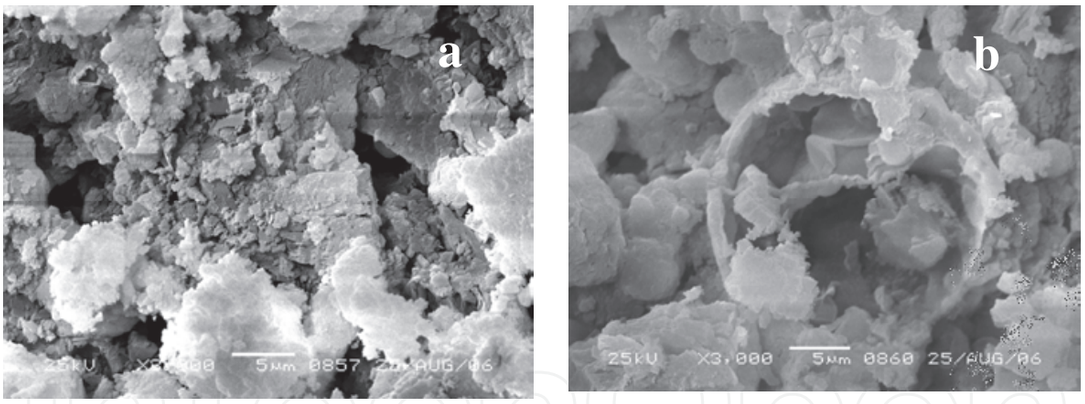

Fig. 10. SEM micrographs of the fracture surface of Al_2O_3/Al composite granules prepared from powdered TCA and PA-4.

However, this process did not lead to destruction of the cermet support granules or substantial mesoporosity degradation (Table 4). According to the data presented in Table 4, the increase of TCA concentration in the initial blend leads to a continuous increase of the specific surface area, volume and average diameter of nanopores.The total pore volume, which, in addition to nanopores, includes macropores and ultramacropores formed by voids between aluminum particles, aggregates of aluminum oxide formed during TCA decomposition and hollow spheres, also increases. Meahwhile, the fraction of nanopores in the total pore volume grows from 44 to 67%. The aluminum precursors alone (see ASD-1 sample with similar properties in Table 2) are not capable of providing for such developed nanopore structure in cermets.

Sample, TCA content in initial blend, wt.%	Specific surface area, m^2/g	Nanopore volume, cm^3/g	Total pore volume, cm^3/g	Average nanopore diameter, nm
60	97	0.25	0.35	7.3
50	87	0.20	0.34	6.8
40	78	0.16	0.33	5.7
30	64	0.12	0.27	5.9

Table 4. Nanopore textural characteristics of granulated composites prepared from powdered TCA and PA-4 (calcination temperature 700°C).

At the same time, the catalytic properties of chromium-alumina catalysts did not change continuously with variation of the TCA concentration in the precursor blend. Maximum isobutene conversion was observed for the sample containing 50% TCA (Fig. 11). This sample is also characterized by the highest selectivity to isobutene. Apparently, this composition has optimum pore structure of the support. In particular it is shown in Fig. 12 that the nanopore structure of the support includes both nanopores with dimensions 3-4 nm (narrow peak) and larger pores with diameters 6-8 nm. The improvement of all nanopore structure parameters is exclusively due to the larger nanopores as the fraction of the smaller ones decreases (Fig. 12). There is certain ratio between the two types of pores in the optimum 50% TCA sample that decreases for the 60% TCA sample (Table 4). It appears that such nanopore structure provides for the optimum structure or size of the catalyst active component.

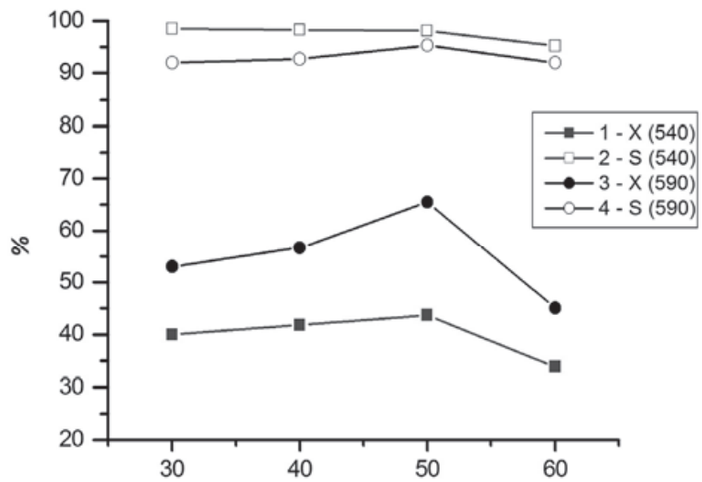

Fig. 11. Dependence of isobutane conversion X (1,3) and selectivity to isobutene S (2,4) at 540°C (1,2) and 590°C (3,4) on TCA concentration (wt.%) in the initial blends used for preparation of granulated composites $CrO_x/Al_2O_3/Al$.

The developed macropore structure of the support granules with 3-5 mm size excludes problems of internal diffusion limitations typical for granulated catalysts. Overall, this provides for high isobutene conversion close to the equilibrium one at this temperature

(Pakhomov, 2006) and unusually high selectivity (>94%) to the dehydrogenation product (Fig. 11).

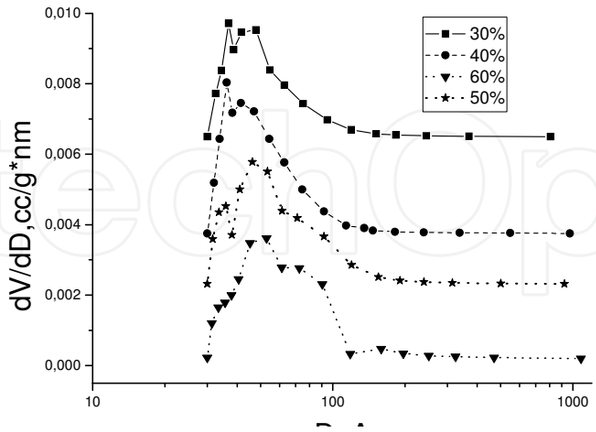

Fig. 12. Nanopore size distribution of Al_2O_3/Al composites prepared from blends with different TCA concentrations.

7. Conclusion

Hydrothermal treatment of blends with aluminum metal powders provides an efficient technique for preparation of mechanically strong monolith composite materials with developed nanopore structure along with a relatively high fraction of macropores. The developed macropore structure provides a high permeability and decreases diffusion limitations inside the porous composite. Changing the reactivity of Al powder particles allows to tune the oxide/aluminum ratio, while their shape affects the monolith permeability. These materials can be used as filters or membrane supports.

Incorporation of precursors of the nanoporous materials in a macroporous system leads to a substantial increase of the nanopore volume. Application of granulated Al_2O_3/Al composites prepared from powdered blends of aluminum and thermally activated gibbsite as catalysts supports allowed us to prepare catalysts with high activity and selectivity in dehydrogenation of isobutane.

8. Acknowledgment

This work was supported by Integrated project of SB RAS and NAS Belorus No 115_3 and T10C-023.

9. References

Balshin, M., (1972), Scientific bases of the powder and fiber metallurgy, Metallurgy Publ. House, Moscow, USSR [in Russian]

Boreskov, G., Dzisko, V., Borisova, M., Krasnopolskaya, V., (1951), „Influence of thermal treatment on the structure and catalytic activity of alumina", Journal of Physical Chemistry, Vol. 26., No. 4., pp.492-499 ISSN 1089-5639 [in Russian]

Fenelonov, V., (2002), Introduction into physical chemistry of formation of supramolecular structure of the adsorbents and catalysts. Publishing house of SB RAS, ISBN-5-7692-0647-0, Novosibirsk, Russia [in Russian]

Gregg, S., Sing, K., (1982), Adsorption, surface area and porosity,: Academic Press, ISBN-10 0123009561, London, United Kingdom

Geguzin, Ya., (1984), Physics of sintering, Nauka, Moscow, USSR [in Russian].

Ismagilov, Z., Shkrabina, R., Koryabkina, N., Kirchanov, A., Verinda, H., Pex, P., (1997), "Porous alumina as a support for catalysts and membranes. Preparation and study", Reaction Kinetics and Catalysis Letters, Vol. 60, No. 1, pp. 225-231, ISSN 0133-1736

Ismagilov, Z., Shepeleva, M., Shkrabina, R., Fenelonov, V., (1991), "Interrelation between structural and mechanical characteristics of spherical alumina granules and the initial hydroxide properties", Applied Catalysis, Vol. 69., No.1., pp. 65-74. ISSN 0926-860X

Khasin, A., (2005), Memrane reactors for the Fischer-Tropsch synthesis, In: "Sustainable Strategies for the Upgrading of Natural Gas: Fundamentals, Challenges, and Opportunities", E.G.Derouane et al. (Eds), 249-271, Springer, ISBN 101-4020-3309-5, Dordrecht, Netherlands

Khalil, K., (1998), „Synthesis of short fibrous boehmite suitable for thermally stabilized transition aluminas formation", Journal of Catalysis, Vol. 178., No.1, pp.198–206, ISSN 0021-9517

Lee, D., Lee, Y., Nam, S., Ohm, S., Lee, K., (2003), "Study on the variation of morphology and separation behavior of the stainless steel supported membranes at high temperature", Journal of Membrane Science, Vol. 220, No1, pp. 137-153. ISSN 0376-7388

Leonov, A., Smorigo, O., Romashko, A., Deshko, M., Ketov, A., Novikov, L., Tankovitch, V., (1998), "Comparative study of the properties of monolith supports of the honeycomb and foam structure for the use in the processes of the catalytic gas purification", Kinetics and Catalysis, 39., 691-700. ISSN 0023-1584

Pakhomov, N., (2006), Modern state and prospects of the dehydrogenation processes. In: Industrial catalysis in lections, Boreskov Indstitute of Catalysis, ISBN 978-5-89530-018-3, Vol. 6., pp. 53-98, Novosibirsk, Russia [in Russian]

Pakhomov, N., Molchanov, V., Zolotovskii, B., Nadtochii, B., Isupova, L., Tikhov, S., Kashkin, V., Kharina, V., Tanashev, Yu., Parakhin. O., (2008), „Development of catalysts for dehydrogenation of C3-C4 paraffins using gibbsite thermal activation product", Catalysis in Industry, Special issue, pp. 13-19, ISSN 1816-0387 [in Russian]

Rat'ko, A., Romanenkov, V., Bolotnikova, E., Krupen'kina, Zh., (2004), "Hydrothermal Synthesis of Porous Al2O3/Al Metal Ceramics: II. Mechanism of Formation of a Porous Al(OH)3/Al Composite", Kinetics and Catalysis, Vol. 45., No. 1., pp. 141-148, ISSN 0023-1584

Rebinder, P., Margolis, L., Schukin, E., (1964), "About mechanical strength of the porous dispersed bodies", Doklady of Physycal Chemistry, 154., 695-700. ISSN 086669-5652 [in Russian]

Rohde, M., Unruh, D., Schaub, G., (2005), "Membrane application in Fischer–Tropsch synthesis reactors—Overview of concepts", Catalysis Today, Vol. 106., No.1, pp. 143-148, ISSN 0920-5861

Sabirova, Z., Danilova, M., Kuzin, N., Kirillov, V., Zaikovskii, V., Kriger, T., Mescheryakov, V., Rudina, N., Brizitskii, O., Hrobostov, L., (2008), "Nickel catalysts on the base of porous nickel for the reaction of methane steam reforming", Kinetics and Catalysis., Vol. 49., No. 2., pp. 449-456, ISSN 0023-1584

Saiz, E., Tomsia, A., (1998), "Kinetics of Metal-Ceramic Composite Formation by Reactive Penetration of Silicates with Molten Aluminum", Journal of American Ceramic Society, Vol. 81., No. 10., pp. 2381-2393, ISSN 0002-7820

Tikhov, S., Fenelonov, V., Sadykov, V., Potapova, Yu., Salanov, A., (2000a), "Porous metalloceramics Al2O3/Al prepared by oxidation of powdered aluminum in hydrothermal conditions. I. Content and macrocharacterisics of composites", Kinetics and Catalysis, Vol.41., No. 3, pp. 907-912, ISSN 0023-1584

Tikhov, S., Zaikovskii, V., Fenelonov, V., Potapova, Yu., Kolomiichuk, V., Sadykov, V., (2000b), "Porous metalloceramics Al2O3/Al prepared by oxidation of powdered aluminum in hydrothermal conditions. II. Content and microtexture of composites", Kinetics and Catalysis, Vol. 41., No.3, pp. 916-922, ISSN 0023-1584

Tikhov, S., Romanenkov, V., Sadykov, V., Parmon, V., Rat'ko, A., (2004a), Porous composites based on oxide-aluminum cermets (synthesis and properties), Publ. House of SB RAS "Geo" Branch, ISBN-5-7692-0705-1, Novosibirsk, Russia

Tikhov, S., Potapova, Yu., Fenelonov, V., Sadykov, V., Salanov, A., Tsybulya, S., Melgunova, L., (2004), "Porous metalloceramics Al2O3/Al prepared by oxidation of powdered aluminum in hydrothermal conditions. IY. Influence of oxide additives on the content and textural properties of composites MOx/Al2O3./Al, Kinetics and Catalysis, Vol. 45., No.2, pp. 642-653, ISSN 0023-1584

Tikhov, S., Potapova, Yu., Sadykov, V., Fenelonov, V., Yudaev, I., Lapina, O., Salanov, A., Zaikovskii, V., Litvak, G., (2005), "Synthesis of alumina through hydrothermal oxidation of aluminum powder conjugated with surfactant-directed oriented growth", Materials Research Innovations, Vol.9., pp. 431-446, ISSN 1432-8917

Tikhov, S., Sadykov, V., Ratko, A., Kuznetsova, T., Romanenkov, V., Eremenko, S., (2007), "Kinetics of aluminum powder oxidation by water at 100°C", Reaction Kinetics and Catalysis Letters, Vol. 92., No.1., pp. 83-88, ISSN 0133-1736

Tsybulya, S.V., Kryukova G.N. (2008). Nanocrystalline transition alumina: Nanostructure and features of x-ray powder diffraction patterns of low-temperature Al2O3 polymorphs, Physical review, Vol.77B, No 024112, pp. 1-13, ISBN 1098-0121

Vityaz, P., Kapcevich, V., Sheleg, V., (1987), "Porous powdered materials and their products", Vysshaya Shkola, Minsk, USSR [in Russian]

Wang, D., Tong, J., Xu, H., Matsumura, Y., (2004), "Preparation of palladium membrane over porous stainless steel tube modified with zirconium oxide", Catalysis Today, Vol. 93-95., pp. 689-693, ISSN 0920-5861

Watari, T., Torikai, T., Tai, W., Matsuda, O., (2000), "Fabrication and mechanical properties of α-Al2O3/β-Al2O3/Al/Si composites by liquid displacement reaction", Journal of Material Science, Vol. 35., No. 2., pp. 515-520, ISSN 0261-8028

Yun, Y., Hong, S., Choi, S., (2002), "Metal penetration processing and mechanical properties of Al/Al2O3 composite system", Journal of Materials Science Letters, Vol. 21., No. 16., pp. 1297-1299, ISSN 0261-8028

Zhu, H., Riches, J., Barry, J. (2002), „γ-Alumina nanofibres prepared from aluminum hydrate with poly(ethylene oxide) surfactant", Chemistry of Materials, Vol. 14., No.8, pp. 2086–2093, ISSN 0897-4756

Zolotovskii, B., Buyanov, R., Bukhtiyarova, G., Taraban, E., Murin, V., Grunvald, V., Demin, V., Sayfullin, R., (1997), "Development of the technology and production of spherical alumina for catalysts supports and adsorbents", Journal of Applied Chemistry, Vol. 70., No.1, pp. 299-306, ISSN 0044-4618 [in Russian]

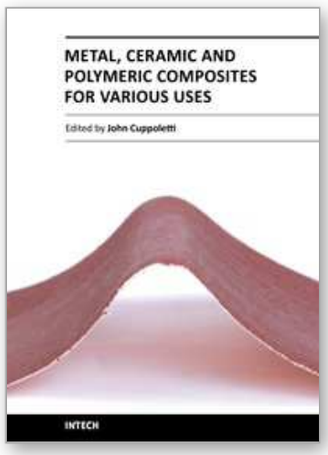

Metal, Ceramic and Polymeric Composites for Various Uses

Edited by Dr. John Cuppoletti

ISBN 978-953-307-353-8
Hard cover, 684 pages
Publisher InTech
Published online 20, July, 2011
Published in print edition July, 2011

Composite materials, often shortened to composites, are engineered or naturally occurring materials made from two or more constituent materials with significantly different physical or chemical properties which remain separate and distinct at the macroscopic or microscopic scale within the finished structure. The aim of this book is to provide comprehensive reference and text on composite materials and structures. This book will cover aspects of design, production, manufacturing, exploitation and maintenance of composite materials. The scope of the book covers scientific, technological and practical concepts concerning research, development and realization of composites.

INTECH
open science | open minds

InTech Europe
University Campus STeP Ri
Slavka Krautzeka 83/A
51000 Rijeka, Croatia
Phone: +385 (51) 770 447
Fax: +385 (51) 686 166
www.intechopen.com

InTech China
Unit 405, Office Block, Hotel Equatorial Shanghai
No.65, Yan An Road (West), Shanghai, 200040, China
中国上海市延安西路65号上海国际贵都大饭店办公楼405单元
Phone: +86-21-62489820
Fax: +86-21-62489821

IntechOpen